Hydrology and
Earth System
Sciences
Discussions

Open Access

Inverse isolation of dissolved inorganic nitrogen yield for individual land-uses from mosaic land-use patterns within a watershed

Y.-T. Shih[1], T.-Y. Lee[2], J.-C. Huang[1], S.-J. Kao[3], K.-K. Liu[4], and F.-J. Chang[5]

[1]Department of Geography, National Taiwan University, Taipei, Taiwan
[2]Department of Geography, National Taiwan Normal University, Taipei, Taiwan
[3]State Key Laboratory of Marine Environmental Science, Xiamen University, Xiamen, China
[4]Institute of Hydrological and Oceanic Sciences, National Central University, Taoyuan, Taiwan
[5]Department of Bioenvironmental Systems Engineering, National Taiwan University, Taipei, Taiwan

Correspondence to: J.-C. Huang (riverhuang@ntu.edu.tw)

Discussion Paper | Discussion Paper | Discussion Paper | Discussion Paper

HESSD

12, 449–487, 2015

Inverse isolation of dissolved inorganic nitrogen yield

Y.-T. Shih et al.

Title Page

Abstract | Introduction

Conclusions | References

Tables | Figures

|◄ | ►|

◄ | ►

Back | Close

Full Screen / Esc

Printer-friendly Version

Interactive Discussion

Full Screen / Esc

Printer-friendly Version

Interactive Discussion

Abstract

This study combines the observed riverine DIN (dissolved inorganic nitrogen) export and the controlling factors (land-use, population and discharge) to inversely estimate the effective DIN yield factors for individual land-use and DIN per capita loading. A total of 16 sub-catchments, with different land-use compositions on the Danshui River of Taiwan, were used in this study. Observed riverine DIN concentrations and yields varied from 20–450 µM and 400–10 000 kg N km^{-2} yr^{-1} corresponding to the increase of urbanization gradient (e.g. building and population). Meanwhile, the transport behaviors changed from hydrological enhancement to dilution with increasing urbanization as well. Our method shows that the DIN yield factors, independent of discharge, are 12.7, 63.9, and 1381.0 µM, for forest, agriculture, and building, respectively, which equals to 444.5, 2236.5, 48 335 kg N km^{-2} yr^{-1} at the given annual runoff of 2500 mm. The agriculture DIN yield only accounts for 10 % of fertilizer application indicating the complicated N cascade and possible over fertilization. The DIN per capita loading (~ 0.49 kg N capita^{-1} yr^{-1}) which is lower than the documented human N emission (1.6–5.5 kg N capita^{-1} yr^{-1}) can be regarded as an effective export coefficient after treatment or retention. A conducted scenario experiment supports the observations demonstrating the capability for assessment. We therefore, can extrapolate all possible combinations of land-use, discharge, and population density for evaluation. This can provide a strong basis for watershed management and supplementary estimation for regional to global study.

1 Introduction

Anthropogenic nitrogen, e.g. fertilizer and excrement, elevated by increasing population and food production, cause serious water and land pollution (Fitzpatrick et al., 2004; Brown et al., 2009; Tu, 2009; Jiang and Yan, 2010). In addition, it causes nitrogen cycle imbalances that already exceed the safe operating parameters for humankind

Full Screen / Esc

Printer-friendly Version

Interactive Discussion

(Downing et al., 1999; Peterson et al., 2001; Rockstrom et al., 2009). This increase of human-related N emission is unlikely to stop and has resulted in eutrophication (Tsai et al., 2013), exacerbation of dissolved oxygen consumption in water bodies (Parr and Mason, 2003), and has also been the cause of human health issues such as *cyanosis* (blue-tinged blood).

Previous global studies on dissolved inorganic nitrogen yields (DIN includes nitrite, nitrate, and ammonium) varies over 3 orders of magnitude from 0.58 to ~ 6000 kg N km^{-2} yr^{-1} among watersheds world-wide (He et al., 2011). These results are highly correlated to population, land-use (e.g. agricultural, commercial or residential) and runoff (Horwarth et al., 1998; Smith et al., 2005; Seitzinger et al., 2005; Horwarth et al., 2006). Meanwhile, nitrogen export from eastern Asia and Oceania is a hotspot due to rapid population growth (Mayorga et al., 2010; Lee et al., 2014). The aforementioned studies broadly shape the picture of global nitrogen export whereas they also point to the regional characteristics and mosaic land-use lead considerable uncertainties on nitrogen export estimations. For example, the sewage treatment efficiency, cultivation types, fertilizer application and environmental background are all regional-dependent. Therefore, extracting the individual output from the land-use-induced effects (e.g. fertilizer application or urban runoff) in a mosaic land-use pattern, which is further complicated by flow paths and processes within watersheds, is a difficult task. To better predict the riverine DIN flux for different scenarios, the individual emission of specific land-use and population should be firstly evaluated.

The riverine DIN output from a watershed is commonly described by the flux or load (a product of the concentration and discharge volume) which is a mixture of all kinds of physical and biological processes interacting with topography, deforestation, urbanization, and hydrodynamics (Fitzpatrick et al., 2005; Bouwman et al., 2013). Thus, previous studies applied multiple regression analysis to estimate riverine DIN concentration and export through the use of dominant factors (e.g. land-use, population and runoff) (Smith et al., 2005, Lee et al., 2014). Other modeling attempts, like PLOAD, Global NEWs, and NANI, compiled export coefficients and parameterizations for individual

sources (including point and non-point) to straightforwardly simulate or estimate the riverine DIN concentration and export (EPA, 2001; Seitzinger et al., 2005; Harworth et al., 1998). Undoubtedly, determination of the export coefficient plays a key role in such relevant applications. Our previous study combined the network of riverine DIN loads to inversely deduce the DIN yield for different land-use categories (Huang et al., 2012). This result is only applicable in the mean state of discharge condition. Moreover, population was not taken into account due to limited population in the study area. We therefore further advanced this concept of inverse estimation onto a larger watershed with a significantly different degree of urbanization and parameterized the stream discharge variability, which has not been considered before, to derive DIN yield factors.

This study monitored 16 sub-watersheds in the Danshui River watershed during 2002–2004. Those sub-watersheds have different mosaic land-use patterns from pristine to the intensively urbanized. Initially, the watershed landscape characteristics, including land-use composition and population density, were delineated. Secondly, the DIN concentration and stream discharge were compiled to calculate the riverine DIN load and yield. Thirdly, the DIN relationships between watershed landscape characteristics were quantitatively determined. Finally, the mosaic land-use pattern and DIN export for those sub-watersheds were superimposed to derive the DIN yield factor for each land-use and the per capita loading. This method, applied to the nested sub-watersheds with different urbanization gradients, can not only aid in understanding the process and the impacts of urbanization on DIN yield but also can be used to quantify the runoff-independent controlling factors.

2 Material and methods

2.1 Characteristics of the Danshui River

The Danshui River flows through Taipei City and is one of the main rivers in Taiwan. The drainage area is 2726 km^2. In this watershed, Taipei City, located downstream, has 6.8

Y.-T. Shih et al.

Title Page

Abstract | Introduction

Conclusions | References

Tables | Figures

◄ | ►

◄ | ►

Back | Close

Full Screen / Esc

Printer-friendly Version

Interactive Discussion

million residences and the population density can reach as high as $\sim 2494\,\mathrm{capita\,km^{-2}}$. The Danshui River has three major tributaries merging in Taipei City. They are the Keelung, Xindian and Dahan Rivers from north to south (Fig. 1). The annual rainfall for the Keelung, Xindian, and Dahan River watersheds are 3750, 4236 and 2742 mm, re-
5   spectively. In general, the wet/dry season (wet season is defined from May to October) rainfall of the three tributaries were 2038/1712, 2739/1497, and 1928/814 mm respectively during 2000–2010 indicating that seasonal variation increases southward. The north east monsoon (October to February in the following year) brings considerable precipitation to Northern Taiwan resulting in the indistinct seasonality in the Keelung
10   River watershed.

     The land-use dataset in this watershed has been provided by the National Land Surveying and Mapping Center (MLSC, 2008). MLSC introduced the aerial photos, satellite imagery, and field survey to identify the 103 land-uses for the entire island and distributed the dataset in 2006. Since this study focuses on the DIN yield, the
15   original land-use types were reclassified into 4 main categories (forest, buildings, agriculture, and water body). The forest class includes natural forest, secondary forest, bamboo land, and shrubs. The agriculture class includes paddies (0.5 % of the whole Danshui basin), dry crops (2.5 %) and tea farms and orchards (2.3 %). Tea farms and orchards mainly occupy the hillside (1000–1200 m a.s.l.). Human-made facilities, such
20   as houses/business buildings (7.0 %), roads (3.7 %), industry factories (1.0 %) and city parks (1.1 %) are classified into the buildings category. Through the reclassification, the forest, buildings, agriculture and water body in Danshui River Basin are 76.7, 13.6, 5.5 and 2.8 %, respectively. Table 1 lists the basic information of sub-catchment characteristics of the Danshui River and the sub-catchments, including landscape attributes,
25   land-use composition and population density. In terms of the land-use pattern, forest is the main land-use for all the catchments (70.8–96.7 %). Building and agricultural land-use spread along the gentle riparian zones of the Danshui River. In the middle stream, some sub-catchments are characterized by intensive agricultural use (e.g. $\sim 23.1\%$ for D02). As expected, the buildings increase from upstream to the downstream area,

Inverse isolation of dissolved inorganic nitrogen yield

Y.-T. Shih et al.

reaching as high as ∼ 20.0 % (e.g. EPA1096). Such a distinct urbanization gradient and numerous land-use compositions provide a good chance to estimate the DIN yield from different mosaic land-use patterns within the sub-catchments.

2.2 Stream discharge and DIN sampling

The stream discharges for the 16 DIN sampling sites are illustrated in Table 2. Nine of the 16 sites have discharge gauges maintained by the Water Resource Agency. For some of the missing measurements, the simulated discharge derived by TOPMODEL was used instead (Huang et al., 2011). For those sampling sites without discharge gauges, their daily discharges were estimated by an aerial ratio method referring to the adjacent discharge gauges (Kao et al., 2004). In general, the annual discharge during 2002 to 2004 for the Danshui River is 1032 to 3229 mm yr^{-1}. The seasonality of stream flow, just like the rainfall, decreases from north to south due to the north east monsoon rains as well. Note, that there was a severe drought that occurred from the summer of 2002 to the summer of 2003 and thus, the stream flow during this period was low. This was particularly apparent during the wet season.

For DIN monitoring, 5 sampling sites were sampled weekly and 5 sites were sampled monthly due to limited manpower. In addition to our own sites, there are an additional 6 sites monitored by the Taiwanese EPA that are monthly sampled and are supplementary to this study (EPA, 2014). For our own sites, the water samples taken from streams in situ were immediately filtered through Whatman® GF/F filters in the field, and the filtrates were quickly frozen in liquid nitrogen for water chemistry analyses. Nitrate, nitrite, and ammonium were determined by ion chromatography (IC), Dionex ICS-1500, with a detection limit of 0.2 µM (Huang et al., 2012; Lee et al., 2014).

2.3 Riverine DIN yield estimation

The riverine DIN yield is defined as the total DIN flux or load normalized by drainage area. The flux or load is the product of substance concentration multiplied by total

discharge volume during a specific period. However, the frequency of substance concentration, compared to the discharge, is much lower than stream discharge. Therefore, different methods have been proposed to supplement the concentration data for flux calculation. In this study, three commonly used methods, linear interpolation (LI), global mean (GM), and flow weighted (FW) have been applied to estimate the DIN flux (Fig. 2).

The LI method linearly interpolates the unmeasured days by the adjacent measurements, and then multiplies by the consecutive daily discharge (Fig. 2a and b). This method is most suitable when the sampling frequency is relatively high. In other words, this method does not explicitly consider the stream-flow effect that occurs when the sampling frequency is low. In these cases, the GM and FW methods are more suited. The GM method multiplies the mean of all sampled substance concentration with the total discharge within the study period to obtain flux. This simple method which does not consider any interaction between concentration and discharge may be the last method in priority, particularly for the lower sampling frequency. The FW method weighs the sampled concentration by discharge. The flux equals the total discharge volume multiplied by the flow-weighted mean of concentration. Comparing the three method (Fig. 2c and d), the GM method seems to under- and over-estimate the flux for enhancement and dilution condition, respectively. Meanwhile, the LI- and FG-derived fluxes are comparable and more accurate than GM-derived result. The advantages and disadvantages of the three methods have been widely discussed (Ferguson, 1987; Preston et al., 1989; Moatar and Meybeck, 2005; Birgand et al., 2010a,b; Lee et al., 2009), but it may not be easy to judge which one is universally suitable for any watershed. The method-choice depends on sampling frequency, hydrological conditions, and substance characteristics. Therefore, we used the average of all the three method-derived fluxes in this study.

2.4 DIN export from land-use and population

As previously mentioned, the observed riverine DIN flux is made up of individual land-use and human emissions. Previous studies addressed the compilation of the dataset (e.g. land-use and population) to straightforwardly estimate the riverine DIN concentration and export, like PLOAD. By contrast, our previous study revealed that this is a feasible way to inversely estimate the export coefficient for individual land-use when the case of observed riverine DIN export is sufficient (Huang et al., 2012). This simplified method shows that riverine DIN flux, in an annual basis, is mainly from land-uses in a mountainous watershed, as following:

$$DIN_{riv,f} = \sum_{i=1}^{n} K_i A_i \tag{1}$$

where $DIN_{river,f}$ indicates the riverine DIN flux ($kg\,N\,yr^{-1}$). K_i and A_i represent the yield ($kg\,N\,km^{-2}\,yr^{-1}$) and area (km^2) for land-use i. In this equation, the yield for individual land-use can be solved when the sub-catchment number of riverine DIN flux is sufficient. In this method, two implicit assumptions are made. One is that the yield should be regarded as an effective export coefficient because the retention or removal processes are assumed steady or completely reacted in an annual scale. Secondly, the in-stream process can be ignored and uniform runoff from all land-uses is also presumed in this study (Gburek and Folmar, 1999; EPA, 2001). Such assumptions are likely valid and acceptable for small watersheds with steep gradients. However, this method does not consider the annual variation of runoff on DIN export and human N emission which is a significant source for urbanized watersheds. To overcome these two disadvantages, the equation can be rewritten as:

$$\frac{DIN_{riv,f}}{A} = DIN_{riv,y} = \sum_{i=1}^{n} C_i R_i P_i + L_p D \tag{2}$$

where $DIN_{riv,y}$ ($kg\,N\,km^{-2}\,yr^{-1}$) is the $DIN_{riv,f}$ normalized by drainage area. P_i (–) is the area fraction for land-use i to the drainage area, A_i/A. R_i is the runoff depth ($mm\,yr^{-1}$) and C_i indicates the DIN yield for unit runoff, equivalent to K_i/R_i. L_p is DIN per capita loading ($kg\,N\,capita^{-1}\,yr^{-1}$). D is population density of a sub-catchment ($capita\,km^{-2}$).

5 This method reallocates the riverine DIN yield from the whole catchment to the DIN emissions from the three major land-use types (forest, agriculture, and building) and human emissions. The parameters land-use proportion (P_i), population density (D), and runoff depth (R_i), can be derived from the observations. Only C_i and L_p should be calibrated for fitting the riverine DIN yields. Note that involving the D and R into this 10 method indicates its capability for assessing the effect of various population densities and runoff conditions. Meanwhile, the seasonal riverine yields should derive the different C_i, considering seasonal variations. Through this simplified model, we can identify the DIN yield from individual land-uses and per capita loading for a mosaic land-use pattern within a watershed.

15 Since uncertainties inevitably exist in the riverine DIN yields, the uncertainties likely propagate to the yield factors and human emission. Thus, the Monte Carlo approach is adopted instead of a linear algebra one. A total of 100 000 random parameter sets were generated by a uniform distribution generator to fit the observed 16 riverine DIN yields. The yield in dry season, wet season and the whole 2003 data were separately used 20 as three dependent variable sets for consideration of seasonality. The RMSE (Eq. 3) and $RMSE_{log}$ (Eq. 4) are designed as target functions. Although RMSE is a good and widely-applied performance measure, the additional performance measure, $RMSE_{log}$,

is more reasonable for the data spanning several orders.

$$\text{RMSE} = \left(\frac{\sum (Y_{\text{obs},i} - Y_{\text{sim},i})^2}{n} \right)^{0.5} \tag{3}$$

$$\text{RMSE}_{\log} = \left(\frac{\sum (\log(Y)_{\text{obs},i} - \log(Y)_{\text{sim},i})^2}{n} \right)^{0.5} \tag{4}$$

where $Y_{\text{obs},i}$ and $Y_{\text{sim},i}$ are the observed and simulated riverine DIN yield, respectively
and n is the sub-catchment number. The two target functions were enforced to be
minimized simultaneously through Pareto-optimal calibration procedure (Gupta et al.,
1998; Khu and Madsen, 2005). Meanwhile, the DIN yields in 2002 and 2004 were used
to validate the calibrated parameters. The results of the DIN yield factors for agriculture,
forests, buildings, and per capita loading for dry season, wet season and the whole
2003 data are presented and discussed.

3 Results

3.1 Spatial patterns of observed DIN concentrations

The mean and SD of DIN concentrations among the 16 sites during 2002–2004 are
shown in Table 3. The DIN concentrations and stream discharge of three sites (K06,
S07 and EPA1908) from upstream to downstream during 2002–2004 are taken as ex-
amples and shown in Fig. 3. Generally, the mean DIN concentrations vary from 18 to
452 µM and it increases dramatically from upstream to downstream. No distinct inter-
annual variation can be found and some sites for the 2004 wet season are not shown
due to limited observations. For the upstream sites (distances larger than 70 km), the
mean DIN concentrations are lower than $< 70\,\mu\text{M}$ (equal to 0.98 mg N/L), and the con-
centration in the wet season is a bit higher than that in the dry season. For downstream

Full Screen / Esc

Printer-friendly Version

Interactive Discussion

Printer-friendly Version

Interactive Discussion

sites, the mean concentrations in both seasons are higher than 200 µM and the concentrations in the dry season are higher than that in the wet season, perhaps indicating a significant dilution or uptake effect. However, the sites in Keelung River are an exception.

The DIN concentrations against land-use are shown in Fig. 4. For the land-use composition, the building area varies from 0.2 to 19.9 % (Fig. 4a), the agriculture area ranges from 0.1 to 23.1 % (Fig. 4b), and the forest area spans from 71 to 97 % (Fig. 4c). In those figures, the DIN concentrations are significantly positively and negatively correlated to building and to forest proportions, respectively. The Pearson's correlation coefficient (ρ) for the DIN concentration between building and forest proportion are as high as 0.81 and −0.75, respectively. Obviously, the land-use composition in sub-catchments strongly affects the riverine DIN concentration in the Danshui River watershed. However, the relationship between the DIN concentration and agricultural use is not as significant as expected ($\rho = 0.26$).

For concentrations and runoff relations, the DIN concentrations against daily runoff of all sub-catchments are shown in Fig. 5. Three sites, K06, S07, and EPA1908, with different degrees of urbanization, are specifically illustrated showing the changes of C–Q relations along the urbanization gradient. The relatively pristine catchment (K06), characterized by high forest cover (96.7 %) and low population density (less than 15.8 capita km^{-2}), showed the lowest DIN concentration (~ 10 µM) and the correlation coefficient between DIN concentration and daily runoff is 0.33 in a log-log scale. This indicates that the DIN concentration is enhanced by runoff in those relatively pristine catchments. In a site with moderate development (S07, the forest cover decreases to 91.8 %), the average DIN concentration was somewhat elevated, but the concentration seems irrelevant to stream discharge since the ρ is as low as 0.22. For the downstream site (EPA1908), the DIN concentration was the highest among the three selected sites. However, the DIN concentration dropped from ~ 400 to ~ 100 µM with the increase of runoff. The ρ value is −0.49 indicating the dilution effect in downstream sites. The results show that the transition of the C–Q relation from the enhancement in pristine sites

to the dilution in the downstream sites where the human activities (high building area and population density) are intensive and extensive.

3.2   Estimation of the DIN yield

Based on the observed concentration and runoff, the DIN yield for each sub-catchment was estimated by the three flux estimation methods (LI, GM, and FW). Figure 6 shows that the ratios of the GM- to LI-derived yield and the FW- to LI-derived yield vary with correlation coefficients between DIN and discharge. It revealed that the GM, compared to LI, tends to overestimate DIN yield while the C–Q relation reveals the dilution conditions, but underestimates the enhancement conditions. In addition, the ratio of FW- to LI-derived DIN yield was scattered for both conditions with a somewhat large bias. Since the sampling frequency, hydrological condition, and substance characteristics lead to various results, the average of the three method-derived fluxes was used to mitigate the systematic (GM to LI) and random (FW to LI) biases.

The DIN yields in the wet and dry season during 2002–2004 are shown in Table 4 and Fig. 7. The DIN yield in dry season increased from 83 to 6806 $kg\,N\,km^{-2}$ along the stream gradient as well as in the urbanization gradient. For the wet season, the yields for sub-catchments also showed an increasing trend, from 226 to 5593 $kg\,N\,km^{-2}$. In general, the annual DIN yield from pristine catchments is less than 800 $kg\,N\,km^{-2}$ (e.g. D13, K06, and K05). In contrast, the yield for downstream catchments can increase to $\sim$ 10 000 $kg\,N\,km^{-2}$ (e.g. K01, EPA1905, and EPA1906). Therefore, among the three tributaries, the yield in the Keelung River is much higher than the other two due to a sharp increase in population and urbanization.

3.3   Land-use DIN yield and human emission

Throughout the method, the DIN yields (including dry-season, wet-season, and 2003 DIN yields) were used to calibrate the 4 parameters (3 land-use yield factors and 1 per capita loading) for each specific time frame as shown in Fig. 8. The yield factors

of forests in dry season, wet season, and annual basis are 7.1, 17.0, and 12.7 µM, respectively. The yield factors for agriculture derived from dry season, wet season, and annual basis are 13.6, 258.4, and 63.9 µM, respectively. The yield factors for buildings from the three specific time frames are 1601.3, 947.7, and 1426.5 µM, respectively. Meanwhile, the human N emissions for the three time frames are 0.57, 0.43, and 0.47 kg N capita^{-1} yr^{-1}. Generally, the forest yields the lowest DIN at the unit runoff among the three land-use parameters. The yield factor in the dry season is even lower, though with a relatively large uncertainty. For agriculture, the DIN yield factor in the dry season is quite low as well, whereas the yields in the wet season are several-fold higher than in the dry season. The DIN yield factor of buildings is much higher than the other two dominating the DIN export. Unlike the other land-uses, the DIN yield factor of buildings for the dry season is almost double as compared to that in the wet season. As for human emission, the per capita DIN loadings remain between 0.43–0.57.

The calibrated DIN yield factors and per capita loading (the annual basis only) were further verified by the 2002 and 2004 data. The performances of model calibration and validation for the 16 sub-catchments are shown in Fig. 9. For the calibration, the R^2 between the simulated DIN yields and the observed ones for all sub-catchments reach a satisfactory value of 0.88 with a regression slope of 0.87 (Fig. 9a). The model performance for validation also shows well-accepted results, having R^2 values of 0.82 with a slope of 0.87 for the entire validation cases pooling seasonal data at all the sites together (Fig. 9b). The agreement between the observed and simulated DIN yields show that the DIN yield factors derived from the inverse isolation are representative according to the wide range of DIN concentration from different urbanization degrees.

Title Page

Abstract · Introduction

Conclusions · References

Tables · Figures

◄ · ►

◄ · ►

Back · Close

Full Screen / Esc

Printer-friendly Version

Interactive Discussion

4 Discussion

4.1 Controlling factor on riverine DIN concentration

DIN concentrations measured at catchment outlets reveal the mixed consequence from mosaic land-use patterns and population densities within catchments. In general, the DIN concentrations of pristine sub-catchments (forest > 96 %) are less than 70 µM, which is comparable with the other pristine watersheds around the world (Huang et al., 2012). In general, the upstream is characterized by high uptake and transformation of DIN (Peterson et al., 2001), thus the DIN delivered less to downstream (Alexander et al., 2000). Therefore, the DIN concentrations in upstream are quite low in pristine lotic environment. With increased human disturbance, the DIN concentrations surge dramatically (Table 3) and ammonia becomes the dominant nitrogen species downstream (Lee et al., 2014). The correlation coefficients between DIN concentration and stream discharge against population are shown in Fig. 10. The correlation coefficients decrease from +0.5 to −0.5 with the increase of population density. For the sub-catchments with sparser population densities, the DIN concentration is positively correlated to stream discharge. By contrast, the DIN concentrations decrease with the increase of stream discharges found at the sub-catchments with dense populations. Note, that with the increasing degree of urbanization, the C–Q relation changes from enhancement to dilution as seen in Figs. 4 and 5.

4.2 Land-use and hydrological control on DIN yield

For DIN yield, the background DIN export for pristine sub-catchments are ∼ 700 kg N km^{-2} yr^{-1} which is consistent with other pristine mountainous catchments in Taiwan (Kao et al., 2004; Huang et al., 2012; Lee et al., 2013). However, it is much higher than other pristine catchments around the world due to abundant precipitation and high atmospheric deposition (Chen et al., 2007; Duce et al., 2008). For cultivated catchments (agriculture area > 10 %), the annual yield rose to 2500 kg N km^{-2} yr^{-1},

about 3.3 times of background yield. In urbanized sub-catchments, the DIN exports surged up to $10\,792.4 \pm 5292.5\,\text{kg N km}^{-2}\,\text{yr}^{-1}$, over 10 times the background yield.

For seasonality, the DIN yields of the all sub-catchments during the wet season are higher than those in the dry season, though the DIN concentrations behave differently. The high DIN yield in the wet season for both hydrological enhancement (pristine) and dilution condition (urbanized) is interesting. The high DIN yield in the wet season can be expected for condition of hydrological enhancement. However, even the DIN concentration is diluted by stream discharge, but if the increase of stream discharge can compensate for the reduction of the DIN concentration, particularly when the discharge surges more significantly, then the yield (product of discharge and concentration) becomes higher as well as shown in Fig. 2b and d. Note, that the seasonality of discharge variation in Keelung River is indistinct due to the north east monsoon in the winter. Thus the seasonality of DIN yields in Keelung River is insignificant. Nevertheless, the elevated DIN yields in the wet season confirm the primary role of stream discharge in DIN export (Smith et al., 2005). Meanwhile, it may also imply that the storage of DIN in a subtropical terrestrial ecosystem is larger than expected, so even with abundant precipitation (e.g. annual precipitation $\sim 2500\,\text{mm}$) it does not flush out completely.

4.3 DIN yield factors for individual land-uses and population densities

The merit of this method is to untangle the individual DIN yield factors from the mosaic land-use pattern in a catchment. The calibrated yield factors, with some uncertainties, can evaluate the riverine DIN export promisingly. In this study, the uncertainty in the forest is probably negligible due to the low deviation of the yield factor. For agriculture, the yield factors for dry and wet season are 13.6 and 258.4 µM, respectively. Given an annual discharge of 2500 mm, the yields are 476 and $9044\,\text{kg N km}^{-2}\,\text{yr}^{-1}$, respectively. The different agriculture yields between the dry and wet seasons may be attributed to the hydrological control, fertilizer application, and planted species. Four aspects must be addressed for understanding the agriculture yield. First, the growing season spans from February to November and fertilizer is applied around December and early July.

The higher discharge in the wet season may be interpreted that the DIN yield of agriculture is 10-fold higher in the wet season than in the dry season. Secondly, the fertilizer application is plantation-dependent. For example, bomb and tea plantations need nitrous fertilizer around $150\,000$ and $78\,650\,kg\,N\,km^{-2}\,yr^{-1}$, respectively (Tsai and Tsai, 2008; Tang, 2010). The various fertilizer applications and plantation characteristics may explain the large uncertainties in the agriculture yield factor. Thirdly, the agriculture N removed from harvest is only approximately $< 15\%$ and only $\sim 12\%$ are exported as riverine DIN (Tsai and Tsai, 2008) indicating the complicated nitrogen cascade which is important in accounting the nitrogen budget of food production. Our estimated yield factor, regarded as effective export coefficient, can be used for exploring the nitrogen cascade in agriculture and calculating the net anthropogenic nitrogen input (Howarth, 1998; Howarth et al., 2006). Finally, since the riverine DIN is significantly elevated, we posit that fertilizer applications could be reduced for preventing over-fertilization.

In urbanized areas, the DIN yield factor of buildings is significantly higher than the other two. This is only the case where the DIN yield factor in the wet season is lower than that in the dry season, indicating hydrological dilution conditions. Lee et al. (2014) revealed that both enhancement and dilution can be found in urban simultaneously. For example, the deposited aerosol (including sulfide, nitrous chemicals and others) on roads and buildings are washed out (Kang et al., 2010). However, the accumulated abundant benthic sludge is transport by high flows (Bernal et al., 1998; Sutton et al., 2000). Although both enhancement and dilution are important in this urban region, the signature of dilution is relatively obvious.

As for the human N emission to riverine DIN export, the average yield is $\sim 0.49\,kg\,N\,capita^{-1}\,yr^{-1}$ with indistinct seasonality, since this parameter is regarded as a point source and is independent with discharge. Van Drecht et al. (2003) collected international data and utilized the GDP to estimate the gross human N emission which varies from 3.7–$5.5\,kg\,N\,capita^{-1}\,yr^{-1}$ (equal to 10–$15\,g\,N\,capita^{-1}\,day^{-1}$). In addition, Lee et al. (2014) compiled documented riverine DIN export and population dataset worldwide to estimate human N emission which they found to be $4.\,kg\,N\,capita^{-1}\,yr^{-1}$.

On the other hand, Smil (2000) concluded that the human N emission corresponding to minimal obligatory is $1.6\,kg\,N\,capita^{-1}\,yr^{-1}$. Those values are higher than our estimated value, $\sim 0.49\,kg\,N\,capita^{-1}\,yr^{-1}$. The difference can be attributed to the different calculation approaches. The aforementioned studies estimated from GDP or attributed all riverine DIN load to the population without the consideration of land-use effect and wastewater treatment. Meanwhile, approximately two-third registered people communicated for their work may result in the lower emission. Since buildings which is highly correlated to population may share some yield from population and the interactions of the two parameters are not easy to separate completely. A similar model, but without the building term, could also simulate the export fairly well ($R^2 = 0.58$). When that was done, the human N emission increased to $3.5\,kg\,N\,capita^{-1}\,yr^{-1}$, which supports our premises. Nevertheless, the reliable estimated yield factors for individual land-use and human emission can be used for assessing land-use change effects on DIN export, though there are some intrinsic uncertainties within the factors.

4.4 Scenario projection

To demonstrate the advantages of this method, four scenarios are proposed. The scenarios contains two population densities (population densities of 50 and $2000\,capita\,km^{-2}$) and two stream discharges ($Q = 1200$ and $3200\,mm\,yr^{-1}$) and the results are illustrated in Fig. 11. All possible combinations of buildings and agricultural use areas are assessed. We also put the 16 observed riverine DIN yields in accordance with the realistic land-use combinations, discharge and population density levels in this figure. In this assessment, the DIN yields increased gently with the decrease of forest, but rapidly with the increase of buildings. As for the change in stream discharge, the discharge has a prevailing effect on the watershed with an intensive building area. The DIN yield increases 2.3 times between two discharge situations, as can be seen in Fig. 11a and b. The DIN yield increases 2.64 times with the same land-use composition. For Fig. 11a and c, we found that population density is a predominant factor for DIN yield. A good example for our scenario assessment is S07 and K01. The two

sub-catchments have similar building/agriculture ratios, but different population densities. The DIN yield, as expected, increases 4× (from 2571 kg N km^{-2} yr^{-1} for S07 to 10 373 kg N km^{-2} yr^{-1} for K01) indicating the merit of this method which can be extrapolated for many specific situations that have not been observed.

Due to population growth, an increase in food demand and urbanization expansions is expected (Fan and Agcaoili-Sombilla, 1997; McCalla, 1998; Foley et al., 2005) and human-induced terrestrial nitrogen input is expected to be exported into the marine environments, eventually (Galloway et al., 2004). Ultimately, urbanization causes an imbalance in the marine coastal nitrogen cycle (Downing et al., 1999) and directly or indirectly affects atmospheric CO_2, and consequently, the climate (Gruber and Galloway, 2008). Therefore, DIN exports are regional-dependent, but with global importance. Our method is needed for those that manage land resources as they attempt to change the land-use within the catchment and assess the environmental impact on a regional scale. Meanwhile, by using some regional supplementary datasets, this model may offer regional estimations of DIN export for global scale studies as well.

5 Conclusions

This study reveals that urbanization associated factors (land-use and population) are the major contributors to the annual mean DIN concentration. Forest and building proportions tightly correlate the DIN concentration negatively and positively, respectively. From the perspective of hydrological control, the transport behaviors transform from enhancement to dilution with the increase of human disturbance and thus hydrology (e.g. discharge volume and seasonal variation) drives DIN exports in this region. According to the inversed estimation of yield factors, the distinctly seasonal yield factor of agriculture land is plantation-dependent and is affected by fertilizer application. This can aid in understanding the nitrogen budget and nitrogen cascade in agricultural lands. Meanwhile, the building yield factor in the wet season is only 50 % less than in the dry season indicating a dominant dilution effect. However, the export can be discharge-dominant

Inverse isolation of dissolved inorganic nitrogen yield

Y.-T. Shih et al.

Full Screen / Esc

Printer-friendly Version

Interactive Discussion

as long as the increase of discharge is abundant enough to defeat the concentration reduction. The lower DIN per capita loading, compared to documented human N emissions from GDP or other methods, may be attributed to it being shared by building or treatment efficiency and thus could be regarded as an effective export coefficient.
5   Finally, this method parameterizes the land-use-specific DIN yield factors and the per capita loading. This provides the basis for assessing possible land-use combinations in different scenarios which is a main concern for watershed management.

References

Alexander, R. B., Smith, R. A., and Schwarz, G. E.: Effect of stream channel size on the delivery of nitrogen to the Gulf of Mexico, Nature, 403, 758–761, 2000.
Bernal, M. P., Navarro, A. F., Sánchez-Monedero, M. A., Roig, A., and Cegarra, J.: Influence of
15   sewage sludge compost stability and maturity on carbon and nitrogen mineralization in soil, Soil Biol. Biochem., 30, 305–313, 1998.
Birgand, F., Faucheux, C., Gruau, G., Augeard, B., Moatar, F., and Bordenave, P.: Uncertainties in assessing annual nitrate loads and concentration indicators. Part 1: Impact of sampling frequency and load estimation alogorithms, T. ASAE, 53, 437–446, 2010a.
20 Birgand, F., Faucheux, C., Gruau, G., Moatar, F., and Meybeck, M.: Uncertainties in assessing annual nitrate loads and concentration indicators: Part 2. Deriving sampling frequency charts in Brittany, France, T. ASAE, 54, 93–104, 2010b.
Bouwman, A. F., Bierkens, M. F. P., Griffioen, J., Hefting, M. M., Middelburg, J. J., Middelkoop, H., and Slomp, C. P.: Nutrient dynamics, transfer and retention along the aquatic
25   continuum from land to ocean: towards integration of ecological and biogeochemical models, Biogeosciences, 10, 1–22, doi:10.5194/bg-10-1-2013, 2013.
Brown, L. R., Cuffney, T. F., Coles, J. F., Fitzpatrick, F., McMahon, G., Steuer, J., Bell, A. H., and May, J. T.: Urban streams across the USA: lessons learned from studies in 9 metropolitan areas, J. N. Am. Benthol. Soc., 28, 1051–1069, 2009.

Chen, X. Y. and Mulder, J.: Atmospheric deposition of nitrogen at five subtropical forested sites in South China, Sci. Total Environ., 378, 317–330, 2007.

Downing, J. A., McClain, M., Twilley, R., Melack, J. M., Elser, J., Rabalais, N. N., Lewis, W. M., Turner, R. E., Corredor, J., Soto, D., Yanez-Arancibia, A., Kopaska, J. A., and Howarth, R. W.: The impact of accelerating land-use change on the N-cycle of tropical aquatic ecosystems: Current conditions and projected changes, Biogeochemistry, 46, 109–148, 1999.

Duce, R. A., LaRoche, J., Altieri, K., Arrigo, K. R., Baker, A. R., Capone, D. G., Cornell, S., Dentener, F., Galloway, J., Ganeshram, R. S., Geider, R. J., Jickells, T., Kuypers, M. M., Langlois, R., Liss, P. S., Liu, S. M., Middelburg, J. J., Moore, C. M., Nickovic, S., Oschlies, A., Pedersen, T., Prospero, J., Schlitzer, R., Seitzinger, S., Sorensen, L. L., Uematsu, M., Ulloa, O., Voss, M., Ward, B., and Zamora, L.: Impacts of atmospheric anthropogenic nitrogen on the open ocean, Science, 320, 893–897, 2008.

EPA, USA: User's Manual of PLOAD version 3.0: An Arcview GIS Tool to Calculate Nonpoint Sources of Pollution in Watershed and Stormwater Projects, US EPA, Washington, DC, 2001.

Environmental Protection Administration (EPA): Environmental Water Quality Information. http://wq.epa.gov.tw/ (21 August 2013), Environmental Protection Administration, Executive Yuan, ROC (Taiwan), 2014.

Fan, S. and Agcaoili-Sombilla, M.: Why projections on China's future food supply and demand differ, Aust. J. Agr. Res. Ec., 41, 169–190, 1997.

Ferguson, R. I.: Accuracy and precision of methods for estimating river loads, Earth Surf. Proc. Land., 12, 95–104, 1987.

Fitzpatrick, F. A., Harris, M. A., Arnold, T. L., and Richards, K. D.: Urbanization influences on aquatic communities in northeastern Illinois streams, J. Am. Water Resour. As., 40, 461–475, 2004.

Fitzpatrick, F. A., Diebel, M. W., Harris, M. A., Arnold, T. L., Lutz, M. A., and Richards, K. D.: Effects of Urbanization on the Geomorphology, Habitat, Hydrology, and Fish Index of Biotic Integrity of Streams in the Chicago Area, Illinois and Wisconsin, Am. Fish. Soc. Symp., 47, 87–115, 2005.

Foley, J. A., DeFries, R., Asner, G. P., Barford, C., Bonan, G., Carpenter, S. R., Chapin, F. S., Coe, M. T., Daily, G. C., Gibbs, H. K., Helkowski, J. H., Holloway, T., Howard, E. A., Kucharik, C. J., Monfreda, C., Patz, J. A., Prentice, I. C., Ramankutty, N., and Snyder, P. K.: Global consequences of land use, Science, 309, 570–574, 2005.

Inverse isolation of dissolved inorganic nitrogen yield

Y.-T. Shih et al.

Title Page

Abstract	Introduction
Conclusions	References
Tables	Figures

◀ | ▶|

◀ | ▶

Back | Close

Full Screen / Esc

Printer-friendly Version

Interactive Discussion

Galloway, J. N., Dentener, F. J., Capone, D. G., Boyer, E. W., Howarth, R. W., Seitzinger, S. P., Asner, G. P., Cleveland, C. C., Green, P. A., Holland, E. A., Karl, D. M., Michaels, A. F., Porter, J. H., Townsend, A. R., and Vorosmarty, C. J.: Nitrogen cycles: Past, present, and future, Biogeochemistry, 70, 153–226, 2004.

Gburek, W. J. and Folmar, G. J.: Flow and chemical contributions to streamflow in an upland watershed: A baseflow survey, J. Hydrol., 217, 1–18, 1999.

Gruber, N. and Galloway, J. N.: An Earth-system perspective of the global nitrogen cycle, Nature, 451, 293–296, 2008.

Gupta, H. V., Sorooshian, S., and Yapo, P. O.: Toward improved calibration of hydrologic models: Multiple and noncommensurable measures of information, Water Resour. Res., 34, 751–763, 1998.

He, B., Kanae, S., Oki, T., Hirabayashi, Y., Yamashiki, Y., and Takara, K.: Assessment of global nitrogen pollution in rivers using an integrated biogeochemical modeling framework, Water Res., 45, 2573–2586, 2011.

Howarth, R. W.: An assessment of human influences on fluxes of nitrogen from the terrestrial landscape to the estuaries and continental shelves of the North Atlantic Ocean, Nutr. Cycl. Agroecosys., 52, 213–223, 1998.

Howarth, R. W., Swaney, D. P., Boyer, E. W., Marino, R., Jaworski, N., and Goodale, C.: The influence of climate on average nitrogen export from large watersheds in the Northeastern United States, Biogeochemistry, 79, 163–186, 2006.

Huang, J.-C., Lee, T.-Y., Kao, S.-J., Hsu, S.-C., Lin, H.-J., and Peng, T.-R.: Land use effect and hydrological control on nitrate yield in subtropical mountainous watersheds, Hydrol. Earth Syst. Sci., 16, 699–714, doi:10.5194/hess-16-699-2012, 2012.

Huang, J. C., Lin, C. C., Chan, S. C., Lee, T. Y., Hsu, S. C., Lee, C. T., and Lin, J. C.: Stream discharge characteristics through urbanization gradient in Danshui River, Taiwan: perspectives from observation and simulation, Environ. Monit. Assess., 184, 5689–5703, doi:10.1007/s10661-011-2374-2, 2011.

Jiang, Y. and Yan, J.: Effects of land use on hydrochemistry and contamination of karst groundwater from Nandong underground river system, China, Water Air Soil Poll., 210, 123–141, 2010.

Kang, J., Cho, B. C., and Lee, C.-B.: Atmospheric transport of water-soluble ions (NO$_3^-$, NH$_4^+$ and nss-SO$_4^{2-}$) to the southern East Sea (Sea of Japan), Sci. Total Environ., 408, 2369–2377, 2010.

Title Page

Abstract | Introduction

Conclusions | References

Tables | Figures

◀◀ | ▶▶

◀ | ▶

Back | Close

Full Screen / Esc

Printer-friendly Version

Interactive Discussion

Kao, S. J., Shiah, F. K., and Owen, J. S.: Export of dissolved inorganic nitrogen in a partially cultivated subtropical mountainous watershed in Taiwan, Water Air Soil Poll., 156, 211–228, 2004

Khu, S. T. and Madsen, H.: Multiobjective calibration with Pareto preference ordering: An application to rainfall-runoff model calibration, Water Resour. Res., 41, W03004, doi:10.1029/2004WR003041, 2005.

Krausmann, F., Erb, K. H., Gingrich, S., Haberl, H., Bondeau, A., Gaube, V., Lauk, C., Plutzar, C., and Searchinger, T. D.: Global human appropriation of net primary production doubled in the 20th century, P. Natl. Acad. Sci. USA, 110, 10324–10329, 2013.

Laaha, G. and Blöschl, G.: Seasonality indices for regionalizing low flows, Hydrol. Process., 20, 3851–3878, 2006.

Lee, T. Y., Huang, J. C., Carey, A. E., Hsu, S. C., Selvaraj, K., and Kao, S. J.: Uncertainty in acquiring elemental fluxes from subtropical mountainous rivers, Hydrol. Earth Syst. Sci. Discuss., 6, 7349–7383, doi:10.5194/hessd-6-7349-2009, 2009.

Lee, T.-Y., Huang, J.-C., Kao, S.-J., and Tung, C.-P.: Temporal variation of nitrate and phosphate transport in headwater catchments: the hydrological controls and land use alteration, Biogeosciences, 10, 2617–2632, doi:10.5194/bg-10-2617-2013, 2013.

Lee, T.-Y., Shih, Y.-T., Huang, J.-C., Kao, S.-J., Shiah, F.-K., and Liu, K.-K.: Speciation and dynamics of dissolved inorganic nitrogen export in the Danshui River, Taiwan, Biogeosciences, 11, 5307–5321, doi:10.5194/bg-11-5307-2014, 2014.

Liu, J., You, L., Amini, M., Obersteiner, M., Herrero, M., Zehnder, A. J. B., and Yangd, H.: A high-resolution assessment on global nitrogen flows in cropland, P. Natl. Acad. Sci. USA , 107, 8035–8040, 2010.

Mayorga, E., Seitzinger, S. P., Harrison, J. A., Dumont, E., Beusen, A. H. W., Bouwman, A. F., Fekete, B. M., Kroeze, C., and Van Drecht, G.: Global Nutrient Export from WaterSheds 2 (NEWS 2): Model development and implementation, Environ. Modell. Softw., 25, 837–853, 2010.

McCalla, A. F.: Agriculture and food needs to 2025, in: International agricultural development, edited by: Eicher, C. K. and Staatz, J. M., JHU Press, 39–54, 1998.

Moatar, F. and Meybeck, M.: Compared performances of different algorithms for estimating annual nutrient loads discharged by the eutrophic River Loire, Hydrol. Process., 19, 429–444, 2005.

National Land Surveying and Mapping Center – MLSC, 2008, "Land Use Investigation of Taiwan", Ministry of the Interior, available at: http://www.nlsc.gov.tw/ (last access: 21 December 2011), Ministry of the Interior, Taiwan, 2008.

Ministry of the Interior: Monthly Bulletin of Interior Statistics, Department of Statistics of ROC, Taipei, Taiwan, 2012.

Parr, L. B. and Mason, C. F.: Long-term trends in water quality and their impact on macroinvertebrate assemblages in eutrophic lowland rivers, Water Res., 37, 2969–2979, 2003.

Peterson, B. J., Wollheim, W., Mulholland, P. J., Webster, J. R., Meyer, J. L., Tank, J. L., Grimm, N. B., Bowden, W. B., Valett, H. M., Hershey, A. E., McDowell, W. B., Dodds, W. K., Hamilton, S. K., and Angelo, S.: Control of nitrogen export from watersheds by headwater streams, Science, 292, 86–90, doi:10.1126/science.1056874, 2001.

Poveda, G., Jaramillo, A., Gil, M. M., Quiceno, N., and Mantilla, R. I.: Seasonally in ENSO-related precipitation, river discharges, soil moisture, and vegetation index in Colombia, Water Resour. Res., 37, 2169–2178, 2001.

Preston, S. D., Bierman, V. J., and Silliman, S. E.: An evaluation of methods for the estimation of tributary mass loads, Water Resour. Res., 25, 1379–1389, 1989.

Rockstrom, J., Steffen, W., Noone, K., Persson, A., Chapin, F. S., Lambin, E. F., Lenton, T. M., Scheffer, M., Folke, C., and Schellnhuber, H. J.: A safe operating space for humanity, Nature, 461, 472–475, doi:10.1038/461472a, 2009.

Rose, S.: The effects of urbanization on the hydrochemistry of base flow within the Chattahoochee River Basin (Georgia, USA), J. Hydrol., 341, 42–54, 2007.

Seitzinger, S. P., Harrison, J. A., Dumont, E., Beusen, A. H. W., and Bouwman, A. F.: Sources and delivery of carbon, nitrogen, and phosphorus to the coastal zone: An overview of Global Nutrient Export from Watersheds (NEWS) models and their application, Global Biogeochem. Cy., 19, GB4S01, doi:10.1029/2005GB002606, 2005.

Smil, V.: Feeding the World, MIT Press, Cambridge, 2000.

Smith, S. V., Swaney, D. P., Buddemeier, R. W., Scarsbrook, M. R., Weatherhead, M. A., Humborg, C., Eriksson, H., and Hannerz, F.: River nutrient loads and catchment size, Biogeochemistry, 75, 83–107, 2005.

Sutton, M. A., Dragosits, U., Tang, Y. S., and Fowler, D.: Ammonia emissions from non-agricultural sources in the UK, Atmos. Environ., 34, 855–869, 2000.

Swaney, D. P., Hong, B., Ti, C., Howarth, R. W., and Humborg, C.: Net anthropogenic nitrogen inputs to watersheds and riverine N export to coastal waters: a brief overview, Curr. Opin. Environ. Sustainability, 4, 203–211, 2012.

Tang, H.-J.: Rational fertilization of green Bamboo. in: Spatial Issue of Cultivation Rational Fertilization, Taichung District Agriculture Research and Extension Station, Council of Agriculture, 149–151, Taichung, 2010.

Tsai, H.-T. and Tsai, Y.-J.: Fertilizer record and application in tea farm. 05-13, Tea Research and Extension Station, 2008.

Tsai, J.-W., Chuang, Y.-L., Wu, Z.-Y., Kuo, M.-H., and Lin, H.-J.: The effects of storm-induced events on the seasonal dynamics of epilithic algal biomass in subtropical mountain streams, Mar. Freshwater Res., 65, 25–38, 2013.

Tu, J.: Combined impact of climate and land use changes on streamflow and water quality in eastern Massachusetts, USA, J. Hydrol., 379, 268–283, 2009.

Van Drecht, G., Bouwman, A. F., Knoop, J. M., Beusen, A. H., and Meinardi, C. R.: Global modeling of the fate of nitrogen from point and nonpoint sources in soils, groundwater, and surface water, Global Biogeochem. Cy., 17, 1115, doi:Curr. Opin. Environ. Sustainability, 2003.

Title Page

Abstract | Introduction

Conclusions | References

Tables | Figures

◄ | ►

◄ | ►

Back | Close

Full Screen / Esc

Printer-friendly Version

Interactive Discussion

Table 1. Watershed characteristics: land-use/pop. density.

Site ID	Tri.	Watershed attributes Distance* (km)	Area (km^2)	Population density (capita km^2)	Land-use composition Agriculture (%)	Forest (%)	Buildings (%)	Water (%)
D13	D	125	118.7	15.8	1.4	96.7	0.2	1.7
D01	D	40	857.5	158.3	4.8	87.7	3.6	3.9
D03	D	39	126.2	488.9	13.1	81.9	4.0	0.9
D02	D	37	53.7	488.4	23.1	70.8	5.0	1.2
EPA1907	D	16	2101.2	1491.9	5.6	82.3	8.9	3.2
K06	K	93	6.7	80.8	1.3	96.4	1.5	0.8
K05	K	90	8.9	81.3	2.3	91.9	4.6	1.2
K01	K	47	203.3	1053.8	2.6	84.0	11.4	2.0
EPA1905	K	32	327.7	1930.3	3.5	79.2	15.4	2.0
EPA1906	K	16	360.5	2617.7	3.2	74.6	19.9	2.2
S07	S	72	110.7	53.7	4.8	91.8	2.0	1.4
S05	S	71	78.9	37.8	2.1	96.0	0.8	1.1
EPA1910	S	40	90.7	644.8	7.5	82.8	8.6	1.1
EPA1908	S	36	106.1	1737.0	7.7	78.1	13.0	1.2
S03	S	34	111.2	1968.6	8.5	76.5	13.9	1.2
EPA1909	S	31	114.6	2060.7	8.2	74.5	16.0	1.2
Danshui River		0	2696.7	2187.1	5.4	77.2	14.1	3.2

* Distance to estuary.

Table 2. Estimated seasonal Discharge for the sampling sites (unit: mm).

Year	2002–2004			2002		2003		2004	
Site ID	Annual	Dry (%)	Wet (%)	Dry	Wet	Dry	Wet	Dry	Wet
D13	1032.7	26.9	72.7	159.4	701.3	223.9	407.0	451.3	1144.5
D01	1232.3	27.4	72.2	237.6	842.4	263.9	474.5	512.6	1352.2
D03	1194.0	27.6	70.5	224.2	525.9	295.0	322.0	549.9	1896.3
D02	1468.1	40.1	58.2	366.4	574.6	566.9	421.1	872.2	1673.7
EPA1907	2107.7	37.3	62.5	551.7	1036.8	630.3	825.7	1171.5	2092.0
K06	2946.4	58.6	41.5	1366.1	966.7	820.2	888.3	2966.7	1815.5
K05	2850.9	58.6	41.5	1321.9	935.4	793.6	859.5	2870.5	1756.7
K01	3231.0	50.2	49.8	1307.8	1142.3	2113.9	1683.3	1444.7	2005.5
EPA1905	3231.0	50.2	49.8	1307.8	1142.3	2113.9	1683.3	1444.7	2005.5
EPA1906	3231.0	50.2	49.8	1307.8	1142.3	2113.9	1683.3	1444.7	2005.5
S07	3229.0	39.5	60.3	870.4	1348.6	1720.2	2534.1	1228.9	1959.8
S05	2243.9	36.8	63.0	449.0	935.2	1294.7	1858.5	724.9	1444.3
EPA1910	1730.1	30.5	69.2	371.0	578.0	637.7	741.4	577.8	2270.5
EPA1908	1726.2	30.5	69.2	370.2	576.7	636.3	739.7	576.5	2265.4
S03	1646.9	30.5	69.2	353.2	550.2	607.0	705.7	550.1	2161.3
EPA1909	1598.9	30.5	69.2	342.9	534.2	589.4	685.2	534.0	2098.5

Table 3. Observed mean DIN concentrations for the sampling sites.

Year Season Site ID	Sample number	CC*	2002–2004 Dry μM	Wet μM	2002 Dry μM	Wet μM	2003 Dry μM	Wet μM	2004 Dry μM	Wet μM
D13	194	0.53	17.9 ± 6.7	24.5 ± 10.7	19.9	27.3	13.8	21.8	22.0	
D01	20	0.34	69.7 ± 57.6	63.1 ± 35.8	35.3	59.3	94.4	67.6	98.2	
D03	20	−0.01	186.1 ± 78.3	164.3 ± 81.4	255.1	188.2	90.9	135.7	134.0	
D02	21	−0.07	154.2 ± 99.3	108.3 ± 45	174.9	113.2	104.6	102.3	107.1	
EPA1907	33	−0.37	431.8 ± 291.5	372 ± 233.9	375.5	455.6	570.0	237.3	401.4	400.6
K06	201	0.33	21.5 ± 5.6	23.3 ± 6.6	22.7	23.0	20.7	23.7	20.5	
K05	200	0.39	22.4 ± 10.5	22.2 ± 11.8	18.4	25.3	27.8	19.2	22.4	
K01	21	−0.18	253.3 ± 119.2	324.1 ± 108.4	244.4	261.7	263.8	386.6	207.1	
EPA1905	33	0.07	217.6 ± 210.8	305.2 ± 173.5	150.0	265.7	431.6	294.6	272.5	353.5
EPA1906	31	0.26	271.7 ± 170.9	314.1 ± 146.4	230.7	328.6	361.0	324.8	218.1	292.6
S07	222	0.22	39.8 ± 14	58.2 ± 19.4	35.4	46.3	47.9	65.9	61.9	77.6
S05	223	0.43	30.8 ± 9	36.4 ± 13.8	31.5	35.1	32.9	37.7	33.6	36.4
EPA1910	33	−0.03	152 ± 85.5	206.3 ± 152.8	120.2	145.1	209.6	127.0	197.3	333.5
EPA1908	33	−0.49	238.4 ± 93.2	218.5 ± 109.8	215.8	232.6	291.1	213.3	169.5	208.7
S03	51	−0.36	302.1 ± 144.2	200.3 ± 82.7	306.1	213.4	205.5	128.4	136.4	
EPA1909	33	−0.48	451.7 ± 242.8	359.9 ± 237.6	408.2	466.2	520.6	360.2	296.9	253.4

* correlation coefficient between DIN concentration and daily discharge in log-log scale.

Table 4. Estimated seasonal DIN yield for the sampling sites (unit: $kg\,N\,km^{-2}$).

Year Site ID	2002–2003 Dry	Wet	2002 Dry	Wet	2003 Dry	Wet	2004 Dry	Wet
D13	47.8 ± 3.6	226.8 ± 7.4	51.0	320.5	44.6	133.1	159.9	–[*]
D01	239.1 ± 113.4	649.6 ± 114.4	141.7	817.0	336.5	482.2	793.1	–
D03	529.7 ± 145.6	1161.9 ± 134.7	658.3	1504.1	401.2	819.8	1253.1	–
D02	654.3 ± 88.6	858.6 ± 131.2	604.8	992.4	703.8	724.9	1663.4	–
EPA1907	3438.7 ± 883.5	4339.6 ± 422	2897.2	5750.3	3980.3	2928.9	5922.8	10 898.0
K06	361.5 ± 125.9	329.2 ± 108.9	463.9	332.4	259.2	326.1	1013.5	–
K05	294.2 ± 22.8	352.4 ± 103.9	291.6	392.0	296.8	312.8	1081.3	–
K01	6607.1 ± 1566.7	5593.2 ± 1417.1	5197.6	3763.2	8016.7	7423.2	3017.6	–
EPA1905	7558.5 ± 4556.4	3523.1 ± 4202.3	3443.3	3248.2	11 673.7	3798.0	4697.7	8737.1
EPA1906	6805.9 ± 2934.6	3816.8 ± 3214	4226.7	3716.4	9385.2	3917.3	4223.9	7345.1
S07	864.6 ± 313	1643.6 ± 313	579.1	984.8	766.7	1534.9	821.9	1604.2
S05	475.4 ± 153.5	746.9 ± 166.9	337.5	539.4	408.9	636.3	254.2	541.9
EPA1910	1029.4 ± 645.4	1325.2 ± 309.6	565.3	1268.1	1493.6	1382.2	1718.8	9615.4
EPA1908	1330.2 ± 386.2	1770 ± 313.3	1030.0	1751.8	1630.4	1788.1	1535.4	6735.0
S03	1195.8 ± 276.6	1456 ± 271.4	1269.3	1496.3	1122.2	1415.7	1462.9	–
EPA1909	1991.1 ± 611.5	3122.8 ± 577.7	1584.6	3408.0	2397.6	2837.7	2631.7	8414.6

[*] DIN concentration observation was stopped in the 2004 wet season.

Figure 1. Landscape of the Danshui River watershed, including land-use pattern, population (red dots) and sampling sites. The empty circle and red square represent water sampling sites and discharge gauge.
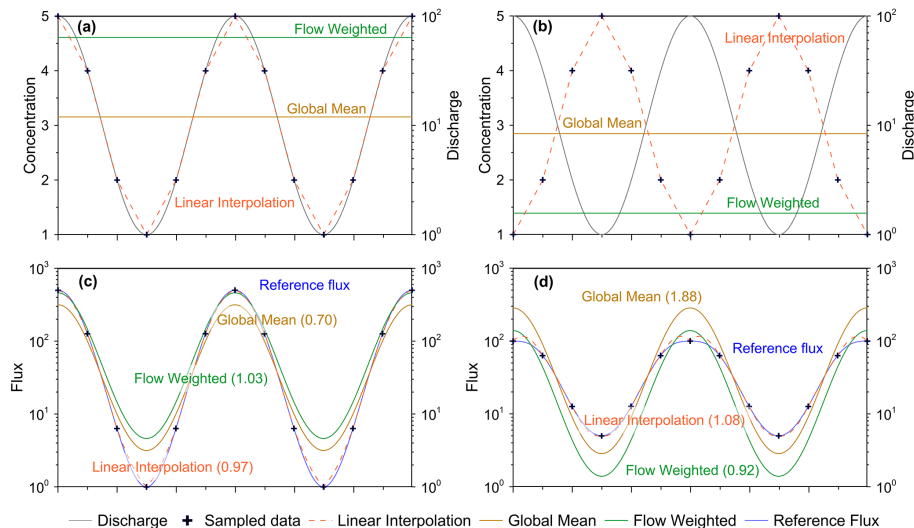
Figure 2. Sketch of three flux estimation methods for hydrological enhancement conditions **(a)** and hydrological dilution conditions **(b)**. The gray line in **(a)** and **(b)** presents discharge. The fluxes derived from the methods are represented in **(c)** and **(d)**, respectively. The value in parentheses means the ratio of total flux between estimated fluxes to reference flux.

Full Screen / Esc

Printer-friendly Version

Interactive Discussion
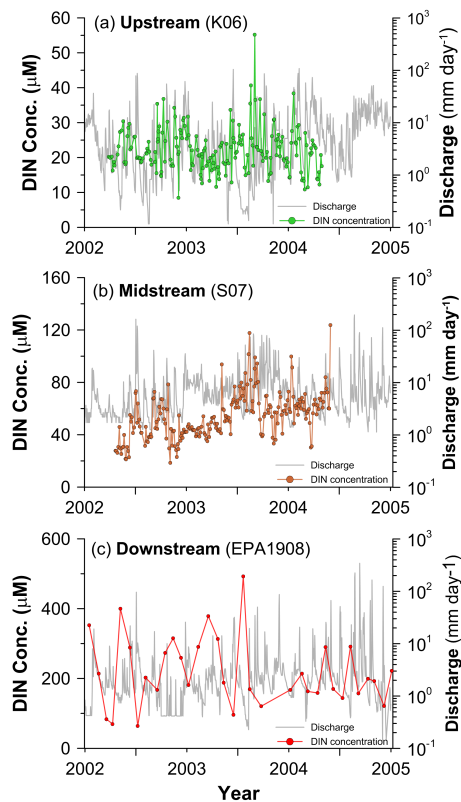
Figure 3. DIN concentrations during 2002–2004. Upstream **(a)**, midstream **(b)**, and downstream **(c)** sites are shown by green (site K06), brown (S07), and red (EPA1908) dots. Stream discharge is represented by gray lines.
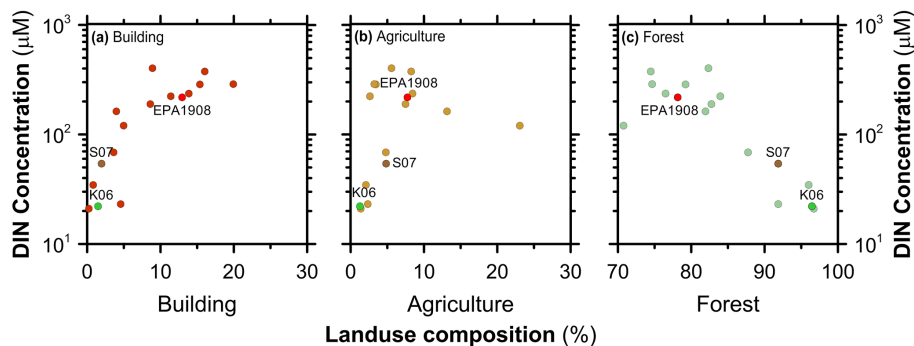
Figure 4. DIN concentration against buildings **(a)**, agriculture **(b)**, and forest **(c)** proportions. Sites K06 (red), S07 (brown) and EPA1908 (red dot) are representatives of upstream, midstream and downstream cases, respectively.
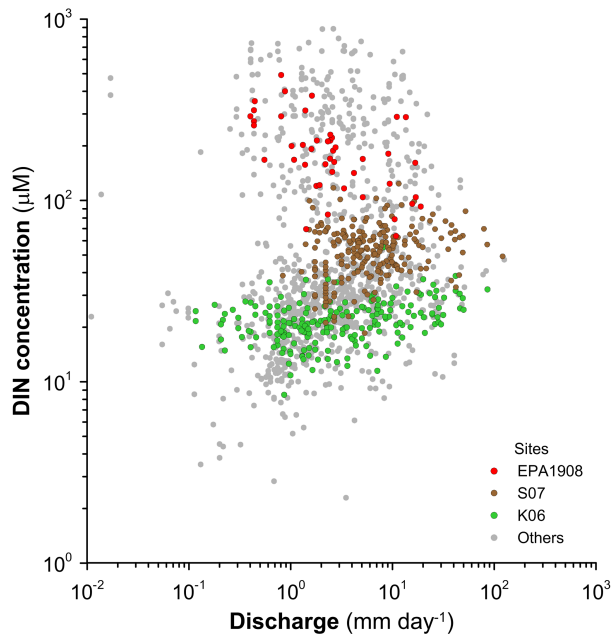
Figure 5. DIN concentrations against stream discharge for all sites during 2002 to 2004. The upstream (K06), midstream (S07), and downstream (EPA1908) sites are represented by green, brown, and red dots.
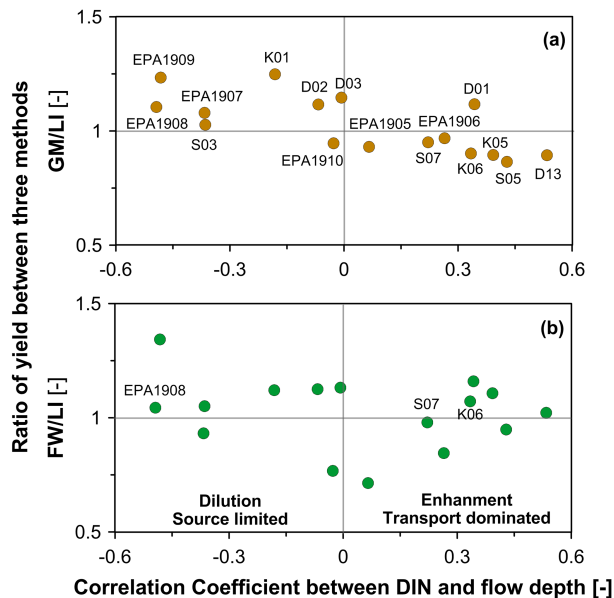
Figure 6. Ratio of three DIN yield estimations against correlation coefficient between DIN conc. and discharge. **(a)** The ratios of GM-derived over LI-derived and FW-derived over LI-derived are illustrated in **(a)** and **(b)**, respectively.
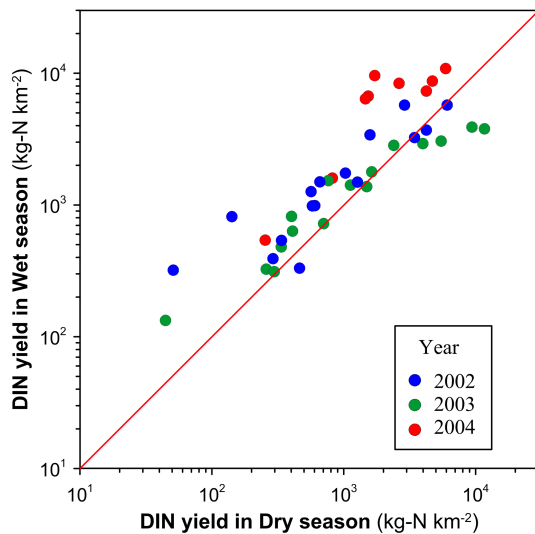
Figure 7. Seasonal variations of estimated yields for all studied sites during 2002–2004.

Full Screen / Esc

Printer-friendly Version

Interactive Discussion

Figure 8. Box plot for model derived parameters: land-use mean concentration and per capita load. The median values of the parameters are presented on the top of the box. Dry season, wet season and annual calibrated processes are filled with brown, blue and green color.
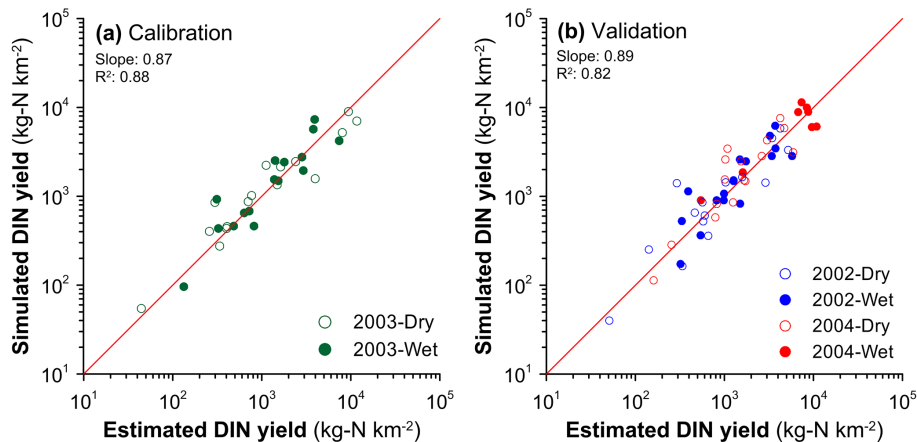
Figure 9. Model performance in calibration **(a)** and validation **(b)**. *x* axis and *y* axis are the estimated and simulated yield. Red line is the slope with 1 : 1 line.
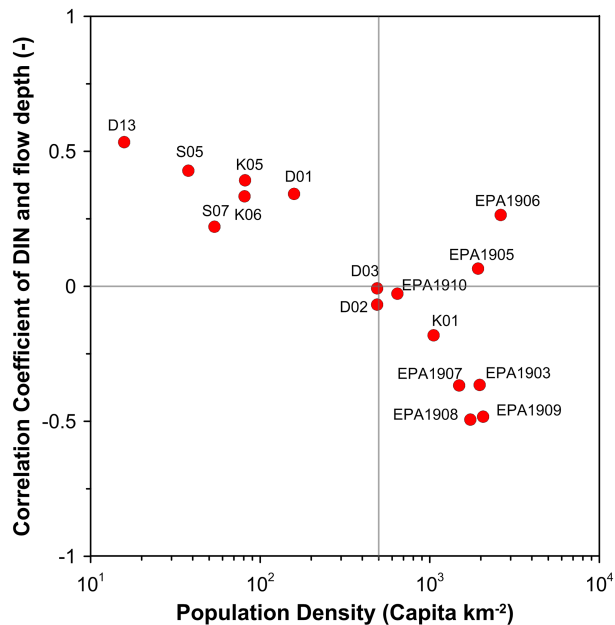
Figure 10. The population effect on hydrological control in DIN concentration.
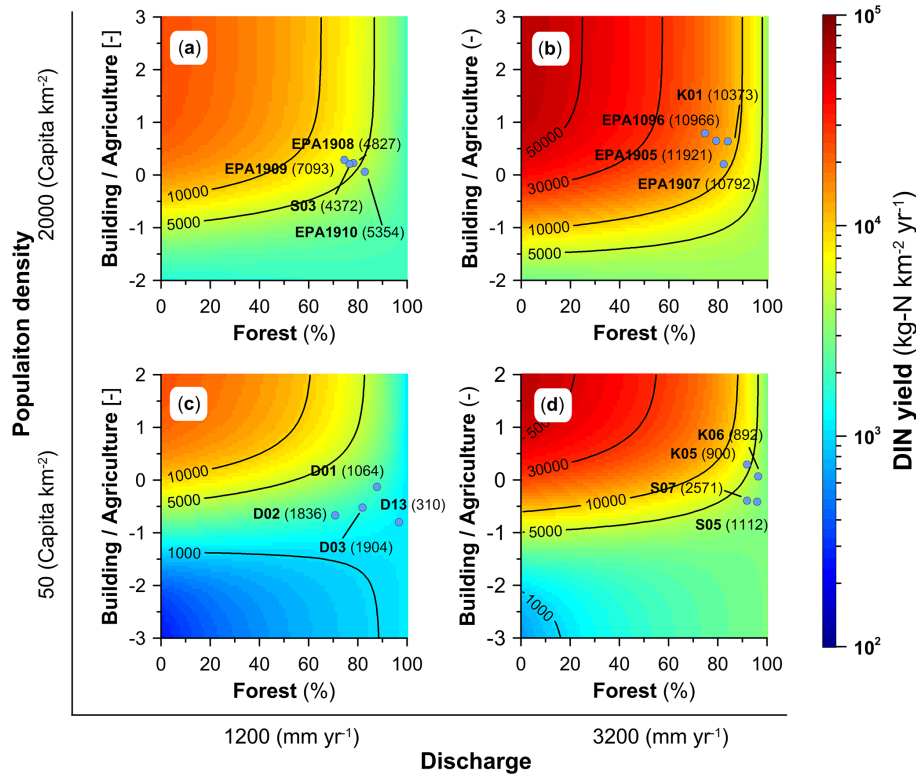
Figure 11. DIN yield with 2 population densities and discharges scenarios. The *x* axis inter subplots is discharge; *y* axis is population density. The intra *x* axis and *y* axis in the subplot are forest and the ratios of building/agriculture are in log scale, respectively. Blue dots are estimated mean yield during 2002–2004 in the Danshui River subcatchments.